EVALUATION OF RT-QUIC DIAGNOSTIC PERFORMANCE FOR CHRONIC WASTING DISEASE DETECTION USING ELK (CERVUS CANADENSIS) EAR PUNCHES

Authors: Bryant, Damani N., Larsen, Roxanne J., Bondo, Kristin J., Norton, Andrew S., Lindbloom, Andrew J., et al.

Source: Journal of Wildlife Diseases, 61(1) : 64-75

Published By: Wildlife Disease Association

URL: https://doi.org/10.7589/JWD-D-24-00071

DOI: 10.7589/JWD-D-24-00071

Journal of Wildlife Diseases, 61(1), 2025, pp. 64–75

Evaluation of RT-QuIC Diagnostic Performance for Chronic Wasting Disease Detection Using Elk (*Cervus canadensis*) Ear Punches

Damani N. Bryant,[1,2] Roxanne J. Larsen,[1,2,5] Kristin J. Bondo,[1,3] Andrew S. Norton,[4] Andrew J. Lindbloom,[4] Steven L. Griffin,[4] Peter A. Larsen,[1,2] Tiffany M. Wolf,[1,3,6] and Stuart S. Lichtenberg[1,2,6]

[1] Minnesota Center for Prion Research and Outreach (MNPRO), University of Minnesota, 1988 Fitch Avenue, St. Paul, Minnesota 55108, USA
[2] Department of Veterinary and Biomedical Sciences, University of Minnesota, 1988 Fitch Avenue, St. Paul, Minnesota 55108, USA
[3] Department of Veterinary Population Medicine, University of Minnesota, 1988 Fitch Avenue, St. Paul, Minnesota 55108, USA
[4] South Dakota Game, Fish and Parks, 523 East Capitol Avenue, Pierre, South Dakota 57501, USA
[5] Current affiliation: Priogen Corp, 1000 Westgate Drive, St. Paul, Minnesota, 55114, USA
[6] Corresponding authors (email: wolfx305@umn.edu; licht213@umn.edu)

ABSTRACT: Sensitive and specific antemortem diagnostic tests are a prerequisite for effective management of chronic wasting disease (CWD). Paired with readily accessible samples that accurately reflect CWD status, the real-time quaking-induced conversion (RT-QuIC) assay has the potential to enable more effective CWD surveillance and interventions. We evaluated the feasibility of RT-QuIC as a CWD diagnostic test using 6-mm ear tissue biopsies from elk (*Cervus canadensis*). First, we evaluated the effect of ear spatial location on seeding activity. We observed an effect of ear punch spatial location on the amyloid formation rate (AFR): Samples collected from the periphery of the ear evidenced a statistically significant increase in AFR relative to ear punches from the ventral midline. Gross microdissection of an ear pinna suggested that there was more small nerve innervation around the periphery of the ear. Second, we evaluated the diagnostic sensitivity, specificity, and predictive value of RT-QuIC using ear punches from elk that had been previously diagnosed via ELISA testing. We evaluated the impact of nonstatistical and statistical approaches on diagnostic accuracy. Specificity and positive predictive value were perfect when statistical analyses were used to evaluate the binomial distribution (CWD positive versus CWD negative) of the data. Conversely, sensitivity and negative predictive value were modest, independent of the application of statistical analysis, indicating that RT-QuIC may be susceptible to false-negative data in this context. Taken together, our data support the idea that RT-QuIC, when paired with US Department of Agriculture–approved diagnostic tests, may provide more time to stakeholders for making major management decisions.

Key words: Amyloid formation rate, antemortem testing, diagnostic concordance, predictive value, prion, sensitivity, specificity, surveillance.

INTRODUCTION

Chronic wasting disease (CWD) is an insidious and invariably fatal neurodegenerative disease of cervids (Williams and Young 1980) that is caused by an infectious misfolded prion protein (Prusiner 1982). The prions of CWD maintain infectivity for extremely long periods of time and have remarkably low infectious doses (Denkers et al. 2020; Kuznetsova et al. 2020). Prions are putatively transmissible via oronasal exposure to environmental vectors such as soil (Johnson et al. 2006, 2007), plants (Pritzkow et al. 2015; Carlson et al. 2023), deer scrapes (Huang et al. 2024), and arthropods (Inzalaco et al. 2023; Soto et al. 2024). As of 1 August 2024, CWD has been detected in free-ranging cervids in 35 US states, four Canadian provinces, Finland (Sun et al. 2023), Norway (Pirisinu et al. 2018), and Sweden (SVA 2024). It has also been detected in captive cervid facilities in 19 states, three Canadian provinces (USGS 2024) and South Korea (Kim et al. 2005; Lee et al. 2013). The spread of CWD across North America is expected to have significant social and economic implications. Furthermore, CWD is a One Health issue, as it has implications for animal health and the environment in addition to its potential impact on human health (Gilch 2022). This disease presents many challenges for

wildlife management agencies (Opsahl 2003; Chiavacci 2022). The worst-case scenario might involve the death of many cervids, resulting in substantial environmental contamination with infectious prions. Social implications include the loss of an important food source and cultural focus for many people, particularly indigenous and rural communities. Although there are no known instances of human CWD zoonosis (Tranulis and Tryland 2023) and the human species barrier appears to be robust (Groveman et al. 2024), the precedent for prion zoonoses exists (Will et al. 1996).

Key tools in the management of any disease are easy-to-use antemortem tests with high diagnostic sensitivity, specificity, and predictive value. Antemortem testing for CWD is a challenging endeavor because of the exceedingly slow progression of prion diseases generally. Body-wide dissemination of infectious prions accelerates in later stages of the disease but is slow initially (Henderson et al. 2020). Furthermore, the relative sensitivities of antibody-based methods (ELISA, western blot) are far lower than would be necessary for antemortem testing of readily accessible tissues (McNulty et al. 2019; Schwabenlander et al. 2022). Antemortem testing for CWD has been met with some success using tonsillar biopsies or rectoanal mucosa–associated lymphoid tissue (RAMALT) by either ELISA or immunohistochemistry (IHC; Wild et al. 2002; Keane et al. 2009; Spraker et al. 2009). However, sampling RAMALT or tonsils antemortem can be highly invasive for the cervid and can be technically challenging for the collector, requiring training as well as veterinary care.

The cervid ear represents an attractive biopsy source, as it is relatively easy to collect. Two publications have evaluated the diagnostic sensitivity and specificity of ear punches using real-time quaking-induced conversion (RT-QuIC; Ferreira et al. 2021; Burgener et al. 2022). RT-QuIC is an extremely sensitive seeded amplification assay that uses fluorescence intensity as a quantitative proxy for the presence of prions in samples of unknown status (Ferreira et al. 2021). Ferreira et al. (2021) reported that mule deer (*Odocoileus hemionus*) and white-tailed deer (*Odocoileus virginianus*) ear punch samples tested with RT-QuIC after iron oxide magnetic bead extraction showed 81% diagnostic sensitivity and 91% diagnostic specificity relative to retropharyngeal lymph node (RPLN) ELISA. Burgener et al. (2022) reported 95% diagnostic sensitivity and 100% diagnostic specificity using white-tailed deer ear punches and belly skin respectively, using traditional RT-QuIC. Taken together, these studies suggest that RT-QuIC testing of ear punches holds promise as an antemortem CWD diagnostic tool for mule and white-tailed deer. To date, no diagnostic evaluation of elk (*Cervus canadensis*) ear tissue has been conducted. Importantly, differences in physiology and disease progression between *Odocoileus* spp. and elk may lead to differences in the relative abundance and subsequent detectability of prions in ear tissue. Earlier work (Race et al. 2007) suggests that prion dissemination in elk is lower than in the *Odocoileus* spp. To address this knowledge gap, we evaluated the diagnostic concordance of RT-QuIC using elk ear punches relative to ELISA-tested obex and/or RPLN from matched animals.

MATERIALS AND METHODS

Sample sources

This study used tissues obtained opportunistically from culling (for population control in areas where hunter harvest is not permitted), hunter harvest, predation, or elk found dead in the Black Hills and other areas in southwestern South Dakota. No animal-use protocol approval was required. In total, 38 elk ear pinnae were received from South Dakota Game Fish & Parks and frozen at −80 C. Specific circumstances of sample collection and demographic details are shown in Supplementary Material Table S1.

Sample preparation

We collected 6-mm ear punches using Integra Miltex disposable biopsy punches (Fisher Scientific, Hampton, New Hampshire, USA) from five locations on each intact ear. The samples generally weighed 100±20 mg. We designated those locations ventral, medial, dorsal, lateral, and central

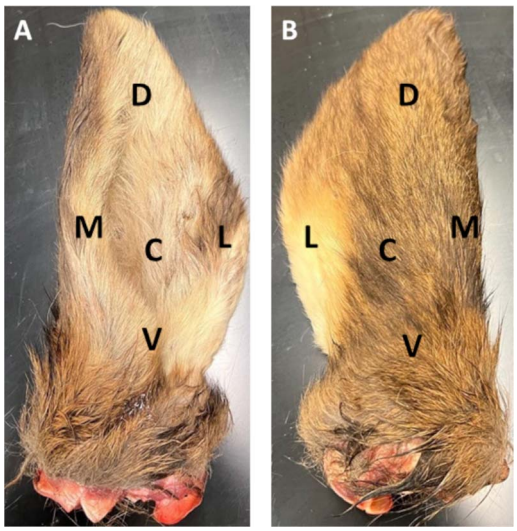

FIGURE 1. (A) Rostral (concave) view of elk (*Cervus canadensis*) ear, left side, and (B) caudal (convex) view of elk ear, left side. Five 6-mm ear punches were made in each ear. Ear punches were designated dorsal (D), lateral (L), ventral (V), medial (M), and central (C).

(Fig. 1). These designations correspond roughly to locations 7, 2, 1, 6, and 5 respectively in Burgener et al. (2022). They correspond to a site intermediate of 2 and 3, 4, 6, 5, and 1 respectively in Ferreira et al (2021). All samples were digested using the protocol described in Burgener et al. Ear punches (~100 mg) were homogenized in 900 µL of a solution of 0.25% w/v collagenase A (Sigma Aldrich, St. Louis, Missouri, USA), 2 mM $CaCl_2$ in 1× phosphate-buffered saline (PBS) using a Beadblaster 24 microtube homogenizer (Neta Scientific, Marlton, New Jersey, USA) with 1.5-mm zirconia beads (Millipore Sigma, Burlington, Massachusetts, USA) for 1 min at 4 m/s. This yielded ~10% (or 10^{-1}) homogenates that were heated and mixed using a ThermoMixer (Eppendorf, Hamburg, Germany) for 24–27 h at 45 C at 700 RPM. Supernatants were collected and frozen at −80 C after the homogenates were centrifuged for 3 min at 3,000 × G. Gross anatomical dissection of the remaining pinnae was performed in a biosafety cabinet using a scalpel and hemostat forceps (Fisher Scientific).

RT-QuIC assay

The RT-QuIC assays were performed as described (Burgener et al. 2022; Schwabenlander et al. 2022). Briefly, ear punch supernatants were diluted to 10^{-2} into RT-QuIC sample dilution buffer, which consisted of 1% N2 supplement (Fisher Scientific) and 0.1% sodium dodecyl sulfate in 1× PBS. Next, 2 µL of the diluted sample was added to 98 µL of RT-QuIC reaction buffer, which consisted of 1× PBS, 500 µM EDTA, 50 µM thioflavin T (ThT), 300 mM sodium chloride, and 0.1 mg/mL recombinant prion protein (rPrP) substrate (MNPROtein; Minnesota Center for Prion Research and Outreach, St. Paul, Minnesota, USA). Eight technical replicates were tested for each ear punch. RT-QuIC assays were run using sealed black 96-well clear-bottom plates (Thermo Scientific, Waltham, Massachusetts, USA) on a FluoStar Omega plate reader (BMG Labtech, Cary, North Carolina, USA). Samples were incubated for 48–49 h with 60 s of double orbital shaking followed by 60 s of rest, for a total of 15 min. A 448-10 excitation filter and a 482-10 emission filter were used to measure ThT fluorescence every 15 min, with a manual gain setting of 1,000. The means of the relative fluorescence intensity units (RFU) of cycles 2 and 3 were used to calculate background fluorescence for each well, in order to control for any RFU variability among wells and to compensate for the greater ThT fluorescence typically found in the first cycle because of viscosity effects (Stsiapura et al. 2008). Cycles 4 onward were normalized to this mean.

Data analysis

The amyloid formation rate (AFR) for each sample was calculated as the inverse of the time to threshold in seconds (calculated as the time required to cross the threshold of twice the background fluorescence), a modification of previously described data processing (Burgener et al. 2022; Schwabenlander et al. 2022) using MARS data analysis software (BMG Labtech). Because there is no consensus on the analysis of RT-QuIC data (Rowden et al. 2023) we first qualitatively described the data. We classified seeding activity across the five punch biopsies of an ear as "strong" or "suspect" (Supplementary Material Table S1). A replicate with "strong" seeding activity generally reached the exponential phase within 6 h of the initiation of the RT-QuIC reaction, similar to CWD-positive lymph node or brain tissue. These reactions were also generally characterized by a fluorescence intensity of 1,000 or more RFU. Conversely, "suspect" seeding activity generally did not reach the exponential phase until 30 h or longer after the

initiation of the RT-QuIC assay and was characterized by sub-1,000 RFU (Supplementary Material Fig. S1).

Nonparametric statistical analysis of ear punch spatial location

Because the AFR data were not normally distributed, we used a nonparametric Kruskal-Wallis H test followed by a Dunn pairwise comparison (Graphpad Prism, Graphpad Software LLC, Boston, Massachusetts, USA) to evaluate the statistical significance of ear punch location.

Nonstatistical assessment

We explored two diagnostic assessments to evaluate the ability of RT-QuIC testing of ear punch samples to discriminate CWD infection status of an elk as defined by ELISA test results of the RPLN and/or obex. For both diagnostic assessments, we used RT-QuIC AFR data from the ear location that had the highest seeding activity as determined from the nonparametric analysis of ear punches from various spatial locations. For the first nonstatistical diagnostic assessment, we designated an ear punch biopsy as CWD positive if 50% (4/8) or more of the RT-QuIC technical replicates evidenced any seeding activity for the duration of the assay (Burgener et al. 2022; Supplementary Material Table S1).

Statistical assessment of binomial distribution using receiver operating characteristic analysis

For the second statistical diagnostic assessment, we conducted a semiparametric receiver operating characteristic (ROC) curve analysis (Pepe 2000) that established an AFR threshold for RT-QuIC positivity. To conduct the ROC analysis, we first normalized AFR values by plate, so the data were in the range (0, 1). We used the following formula to normalize the AFR values by plate:

$$Xscaled = X - x\min/x\max - x\min$$

where *Xscaled* is the normalized AFR value, *X* is the AFR value for each technical replicate of each elk ear biopsy on a given plate and *x*min and *x*max are the minimum and maximum AFR values respectively of all technical replicates of elk ear biopsies on a given plate.

To obtain fitted values for the ROC analysis, we fit the median of the normalized AFR values into a generalized linear model with a binomial distribution and logit link function,

$$\log(\mu/1 - \mu) = \beta_0 + \beta_1 x_1,$$

where μ represents the log odds of the ELISA test having a positive test result (coded as 0, negative, or 1, positive), β_0 is the intercept of the model, and β_1 is the coefficient associated with the predictor variable, x_1, which is the median of the normalized AFR values. We determined the optimal threshold for AFR associated with an optimal combination of sensitivity and specificity from area under the curve (AUC). We used the pROC package (Robin et al. 2011) in R statistical software (R Core Team 2024) to plot ROC and determine AUC.

Assessment of diagnostic test performance

We evaluated each method of assessing the binomial distribution (statistical and nonstatistical) by calculating sensitivity, specificity, positive predictive value (PPV), and negative predictive value (NPV). We calculated these metrics as described by Dohoo et al. (2009) in comparison with ELISA of obex and/or RPLN. We estimated sensitivity as the number of elk positive by both tests divided by the total number positive by ELISA and specificity as the number negative by both tests divided by the total number negative by ELISA. We calculated PPV, or the probability that an elk that tests positive by RT-QuIC of an ear punch is also positive by ELISA (of obex and/or RPLN), as the number of elk positive by both tests divided by the total number of elk positive by RT-QuIC. We calculated NPV, or the probability that an animal negative by RT-QuIC is also negative by ELISA, as the number of elk negative by both tests divided by the total number of elk negative by RT-QuIC. We calculated exact 95% confidence intervals (CIs) for binomial counts or proportions using the epi.R package (Carstensen et al. 2023).

To determine the level of agreement beyond chance between ELISA and RT-QuIC to discriminate the presence of CWD prions at the animal level, we computed McNemar test, kappa statistics, and 95% CIs for each diagnostic assessment using the epi.R package. If the McNemar test was significant or prevalence was <20 or >80%, we reported the prevalence-adjusted and bias-adjusted kappa statistic (PABAK; Sim and Wright 2005). Otherwise, we reported the Cohen kappa statistic (KAPPA). The strength of agreement was classified using the criteria described for kappa

statistics by Landis and Koch (1977), which considered kappa statistics of 0.41–0.60 to be moderate agreement, 0.61–0.80 to be substantial agreement, and greater than 0.81 to be almost perfect. Statistical tests were considered significant at $\alpha=0.05$.

RESULTS

Specific details about ELISA (TeSeE Kit, Bio-Rad, Hercules, California, USA) testing and diagnosis are indicated in Supplementary Material Table S1. The ELISA data from the three diagnostic laboratories indicated that 18/38 (47%) of the elk tested were CWD positive. Of these, 15/18 (83%) exhibited strong (RFU>1,000) RT-QuIC seeding activity (Supplementary Material Table S1). Of the 20 ELISA-diagnosed CWD-negative elk, one biological replicate (5%) exhibited strong RT-QuIC seeding activity. All 10 of the animals designated Wind Cave National Park Surveillance (Supplementary Material Table S1) were culled and exhibited suspect (RFU<1,000) seeding activity. Two of the four animals designated "research" had been found dead: One of these was a coyote predation victim and the other was of unknown status. Four of the five (75%) animals designated "sick/surveillance" were ELISA-diagnosed positive and RT-QuIC positive; the fifth was ELISA-diagnosed negative and RT-QuIC negative. No further details were available to us for sick/surveillance animals. The remaining elk were collected via hunter harvest.

A Kruskal-Wallis H test of ELISA-diagnosed CWD-positive (only) ear punch AFR data indicated a statistically significant effect of spatial location ($H=14.95$, $P=0.0048$). Post hoc Dunn tests indicated a statistically significant reduction in the ventral punch AFR relative to medial (mean rank difference=−96.49, $P=0.0067$), dorsal (mean rank difference=−81.75, $P=0.0396$), and lateral (mean rank difference=81.71, $P=0.0398$) ear punches (Fig. 2). Based on these data, and because few people would simultaneously collect five ear punches per elk in practice, we performed a nonparametric analysis and semiparametric analysis on the medial ear punches only Nonparametric statistical analysis of all of our data showed a statistically significant reduction ($P=0.0067$, 0.0396, 0.0398 respectively) in the AFR of samples collected from the ventral area of the elk ear, relative to medial, dorsal and lateral areas. A statistically nonsignificant reduction in AFR ($P=0.9288$) was also observed in the central punch.

Supplementary Material Table 2 shows the sensitivity, specificity, PPV, and NPV of RT-QuIC relative to ELISA, using the 50% of 40 technical replicates threshold; i.e., across all technical replicates and spatial locations per elk ear). All other spatial comparisons were statistically insignificant. We found that 15/38 elk were CWD positive based on seeding in 50% of the eight replicates of the medial ear punch location. A total of 12/38 elk were classified as CWD positive based on the median AFR threshold for detection established by the ROC analysis. Using the seeding in 50% of the eight technical replicates approach, RT-QuIC had a sensitivity of 67% (95% CI, 41.0–86.7%), a specificity of 85% (95% CI, 62.1–96.8%), a PPV of 80% (95% CI, 51.9–95.7%), and an NPV of 74% (95% CI, 51.6–89.8%; Table 1). The threshold of the median normalized AFR was 0.2198, and AUC was 78.3%. Using ROC analysis, RT-QuIC had a sensitivity of 67% (95% CI, 41.0–86.7%), a specificity of 100% (95% CI, 83.2–100%), a PPV of 100% (95% CI, 73.5–100.0%), and an NPV of 77% (95% CI, 56.3–91.0%; Table 2).

When comparing detection of CWD prions between ELISA and the RT-QuIC method based on seeding in 50% of the eight technical replicates of the medial ear punch location, McNemar test was not significant ($\chi^2=1.00$; $P=0.317$), and KAPPA was 0.52 (0.25–0.79), indicating moderate agreement between the two methods. When comparing detection of CWD prions between ELISA and ROC, McNemar test was significant ($\chi^2= 6.00$; $P=0.014$), and PABAK was 0.68 (0.37–0.88), indicating substantial agreement between the two methods.

On the caudal (i.e., convex) surface of the pinna there were two main cartilage ridges and three visible neurovascular bundles. Figure 3A

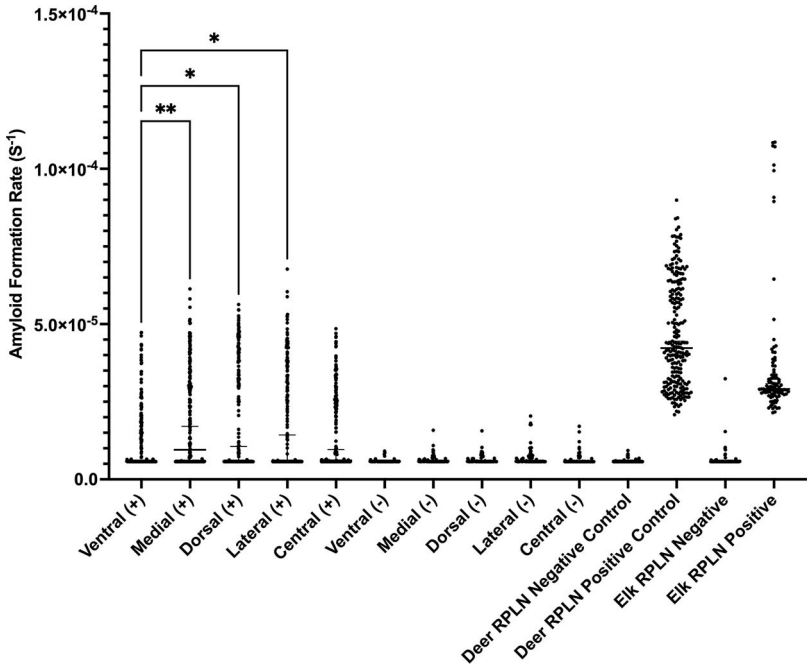

FIGURE 2. Amyloid formation rate (entire real-time quaking-induced conversion run) of elk ear punches sorted by spatial location and ELISA status. Five spatially distinct samples were collected from each of 38 biological replicates. Eight technical replicates were run for each sample. ELISA-diagnosed chronic wasting disease (CWD)–positive (n=18 biological replicates) and CWD-negative ear punches (n=20 biological replicates) are indicated by + and −, respectively. ELISA-diagnosed CWD-positive (n=12) and CWD-negative (n=14) elk retropharyngeal lymph nodes (RPLNs) are also plotted for comparison. The median and 95% confidence interval are indicated by horizontal bars. Deer CWD-positive and CWD-negative plate controls are subsampled from 1 biological replicate each. A Kruskal-Wallis H test of ELISA-diagnosed CWD-positive ear punches was statistically significant (H=14.95, P<0.0048). Post hoc Dunn tests indicated a statistically significant reduction in the ventral punch AFR relative to medial (**mean rank difference =−96.49, P=0.0067), dorsal (*mean rank difference=−81.75, P=0.0396) and lateral (*mean rank difference=81.71, P=0.0398) ear punches. All other post hoc comparisons of ELISA-diagnosed, CWD-positive samples were statistically insignificant.

provides the clearest visualization of the ear punch locations on the caudal surface of the pinna. At the base of the pinna, there were three to four locations where neurovascular bundles entered the auricular cartilage (Fig. 3B, C).

DISCUSSION

Based on our data, we recommend the application of ROC curve analysis to AFR data in order to obtain the best achievable RT-QuIC diagnostic accuracy. This recommendation is based on our evaluation of the sensitivity, specificity, and predictive value of RT-QuIC testing of elk ear punches in the context of CWD diagnosis. Sensitivity and specificity are calculated to evaluate diagnostic performance, whereas predictive value is calculated to predict the likelihood that, given a certain test result, the subject does or does not have the disease (Monaghan et al. 2021). In contrast to sensitivity and specificity, which are a function of the test itself, predictive value varies as a function of disease prevalence, such that PPV increases and NPV decreases when disease prevalence increases.

In our study, ELISA of the obex and/or RPLN results were represented as "true disease" status. There is a possibility that an animal may be classified as negative because of a nondetect using ELISA with RPLN while still actually being CWD positive. This could arise because of the animal being in the earliest

TABLE 1. Sensitivity, specificity, positive predictive value (PPV), and negative predictive value (NPV) of chronic wasting disease (CWD) diagnosis using real-time quaking-induced conversion (RT-QuIC) on elk (*Cervus canadensis*) ear biopsies, with 50% of 8 medial biopsy technical replicates (any seeding activity in 4/8 technical replicates) established as the threshold for RT-QuIC diagnosis of CWD positivity. Sensitivity, specificity, and predictive value were subsequently calculated relative to the ELISA data as a reference standard.

	RT-QuIC	
	Positive	Negative
ELISA		
Positive	12	6
Negative	3	17
Sensitivity, % (95% CI)	66.7 (41.0–86.7)[a]	
Specificity, % (95% CI)	85.0 (62.1–96.8)	
PPV, % (95% CI)	80 (51.9–95.7)	
NPV, % (95% CI)	73.9 (51.6–89.8)	

[a] CI = confidence interval.

TABLE 2. Sensitivity, specificity, positive predictive value, and negative predictive value of chronic wasting disease (CWD) diagnosis using real-time quaking-induced conversion (RT-QuIC) on elk (*Cervus canadensis*) ear biopsies, with a semiparametric receiver operating characteristic (ROC) analysis used to establish the threshold for RT-QuIC diagnosis of CWD positivity. Sensitivity, specificity, and predictive value were subsequently calculated relative to the ELISA data as a reference standard.

	RT-QuIC	
	Positive	Negative
ELISA		
Positive	12	6
Negative	0	20
Sensitivity, % (95% CI)	66.7 (41.0–86.7)	
Specificity, % (95% CI)	100 (83.2–100)	
PPV, % (95% CI)	100 (73.5–100)	
NPV, % (95% CI)	76.9 (56.3–91)	

[a] CI = confidence interval.

stages of disease progression, reduced prion trophism in elk relative to deer (Race et al. 2007), the somewhat low sensitivity of ELISA (at least compared to seeded amplification assays), or the lack of obex for testing. The temporal gap between detectability in RPLN vs. obex is reasonably small and is only present in about 12% of animals (Spraker et al. 2004). Keeping the aforementioned caveat in mind, we observed no false-positive data using the ROC-established threshold for CWD positivity: A positive test using ROC curve analysis to determine the binomial distribution (CWD positivity) correctly identified subjects with CWD. Our ROC PPV data indicated that subjects that returned a positive RT-QuIC ear punch were highly likely to have a positive obex and/or RPLN by ELISA. These data are consistent with prior publications that observed 91% and 100% specificity in RT-QuIC testing of ear punches from white-tailed and mule deer (Ferreira et al. 2021) and white-tailed deer (Burgener et al. 2022), respectively. Conversely, we did observe false-positive data in the nonstatistical 50% of technical replicates approach, indicating that this analysis is suboptimal for management decision-making: 3/20 ELISA-diagnosed negative animals were designated CWD positive by RT-QuIC using this approach.

The RT-QuIC testing of elk ear punch biopsies may be susceptible to false-negative data. We found that the statistical approach was a slight improvement over the nonstatistical approach. A 74–77% NPV indicates a 23–26% chance that a subject diagnosed CWD negative by ear punch biopsy using RT-QuIC may actually be CWD positive by ELISA of the obex and/or RPLN. Sensitivity using ear punch biopsy RT-QuIC (67%) was comparable to testing of RAMALT by RT-QuIC and IHC in elk (Haley et al. 2016). Under conditions of relatively low sensitivity, it may be worthwhile to employ various tactics such as more extensive sampling of the ear, enhanced (iron oxide magnetic extraction) RT-QuIC assays (Ferreira et al. 2021), and US Department of Agriculture (USDA)–approved tests such as ELISA or IHC using RPLN or obex. Along these lines, the qualitative descriptions "strong" and "suspect" were employed in the current study to evaluate data that incorrectly

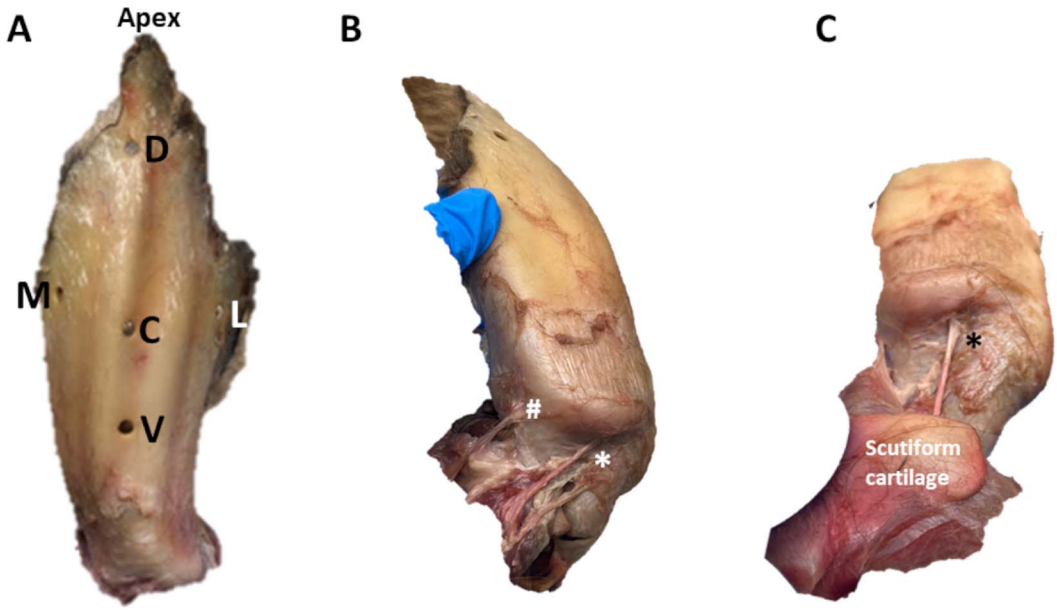

FIGURE 3. Ear biopsy sampling locations on the auricular cartilage of a right elk (*Cervus canadensis*) pinna. (A) An image of the caudal surface (convex) of the auricular cartilage after removal of hair and skin showing the biopsy locations dorsal (D), lateral (L), ventral (V), medial (M), and central (C). Note the two prominent ridges and three depressions where neurovascular bundles were found. (B) Medial border of right ear and (C) ventromedial view at the base of auricular cartilage—both show neurovascular bundles (indicated by the hashtag # and asterisk *) entering the cartilage. The scutiform cartilage is also labeled.

(i.e., fail to) meet the threshold for significance using statistical or nonstatistical approaches. For example, elk 38 was ELISA-diagnosed CWD positive but RT-QuIC negative by statistical and nonstatistical analysis. Looking at the "strong" (>1,000 RFU) seeding activity, an analyst might designate it RT-QuIC positive, assuming that it is early in the disease progression. In contrast, elk 42 evidenced "strong" seeding activity but was diagnosed negative by ELISA and RT-QuIC. Interpretation of RFU values generated by RT-QuIC in the absence of other metrics (AFR, maximum slope, maximum point ratio, etc.) is basically impossible. To date there has been no definitive analysis of what exactly is represented by maximum RFU values or if these values are representative of any biological phenomenon at all. In our laboratory, we generally see what we call "strong" RFU values associated with true-positive samples, but this is by no means universal across all samples, or even across replicates at times. This inconsistency renders interpretation of RFU values alone mostly moot. Despite having sufficient statistical power, our data highlight diagnostic uncertainty that remains in the face of the most sensitive assays.

Given the profound implications of CWD management, stakeholder confidence in CWD diagnostics is important. RT-QuIC has yet to be formally approved by the USDA as a test for diagnosing CWD, and its findings should be interpreted cautiously. Limitations to this assay include lack of consensus on the analysis and interpretation of its data (Rowden et al. 2023). Our study advances this conversation by documenting improved RT-QuIC diagnostic accuracy when ROC curve analysis is used to determine the binomial distribution of unknown samples. The value proposition of RT-QuIC is that it increases antemortem diagnostic access, providing stakeholders with more time to be careful and precise with decision-making. We are unaware of any published evidence of successful ELISA or IHC

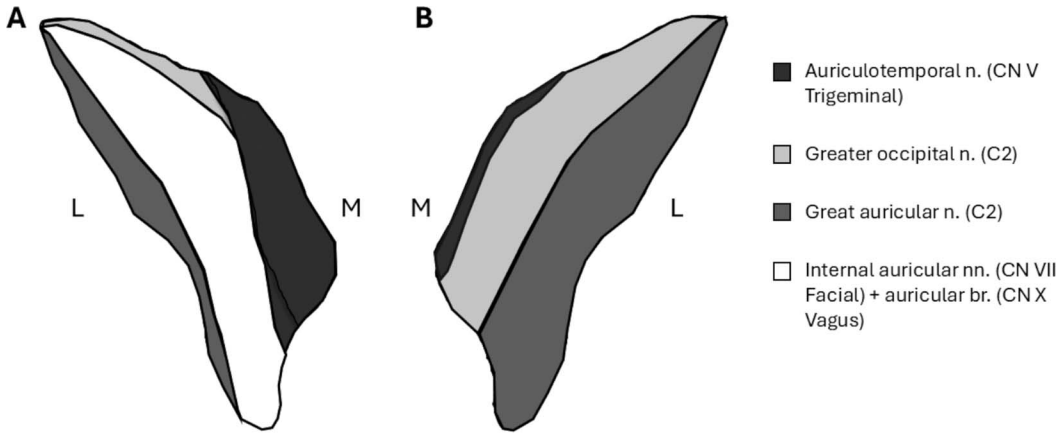

FIGURE 4. Diagram showing the predicted distribution of sensory nerves of a right elk (*Cervus canadensis*) ear. (A) Rostral (concave) view with four nerves from lateral (L) to medial (M): great auricular nerve (n.), internal auricular n., greater occipital n., auriculotemporal n. (B) Caudal (convex) view with three nerves from M to L: auriculotemporal n., greater occipital n., great auricular n.

diagnosis of CWD using ear punches or skin. Current USDA approved ELISA and IHC tests require obex or RPLN for definitive CWD diagnosis (USDA, Animal and Plant Health Inspection Service, 2024). Although RAMALT and tonsil have been successfully tested antemortem (Wild et al. 2002; Keane et al. 2009; Spraker et al. 2009), they are technically challenging to collect and are highly invasive. Given the high specificity and PPV documented by this study and the nascent literature (Ferreira et al. 2021; Burgener et al. 2022), RT-QuIC analysis of punches from any ear location is an easy and useful first step for evaluating the CWD status in cervids.

A secondary aim of this study was to evaluate the extent to which anatomical features influenced results. Spatial differences in RT-QuIC seeding activity are likely explained by prion neurotropism and differences in nerve innervation patterns. There are few anatomical descriptions of the cervid ear in the literature (Rashid et al. 1987). The most relevant literature used was centered on bovine (Budras and Habel 2011) and canine ear anatomy (Evans and de Lahunta 2012). The pinna and any neurovascular bundles (i.e., veins, arteries, and nerves) entering or exiting the ear were the focus, as these structures follow each other as they branch to reach tissues. It is likely that the largest branches of nerves are found at the base of the pinna (most ventrally), and that branches become smaller as the nerves reach the medial and lateral edges and apex of the pinna. Previous studies have shown that the auricular cartilage has several neurovascular branches running within the cartilage and its ridges (Rashid et al. 1987). These are probably where the nerves of the rostral (concave) surface enter to provide sensory innervation of the pinna and the external ear canal. There are four main nerves related to sensory innervation of the pinna. These nerves include branches of three cranial nerves: the trigeminal (auriculotemporal with rostral auricular and external acoustic branches), facial (several internal auricular branches), and vagus (auricular branch), as well as the second cervical nerve (great auricular and greater or major occipital nerves; Budras and Habel 2011; Evans and de Lahunta 2012). The predicted rostral and caudal distribution of these nerves is shown in Figure 4A, B. An in-depth study of comparative ear anatomy across cervids should be a next step to determine if neurovascular patterns are consistent, which could increase sampling efficacy. Additionally, it is likely that auricular branches of the vagus nerve are also intermingled with the facial nerve branches that are found in the external ear canal (Budras and

Habel 2011; Evans and de Lahunta 2012). This could be significant in that the vagus nerve, and potentially other cranial nerves (e.g., facial) are associated with the autonomic nervous system pathways, which play a large role in transport and neuroinvasion of prions in the body (Seelig et al. 2011).

Although Ferreira et al. (2021) reported higher seeding activity from punches around the central nerve of the mule/white-tailed deer (areas 1, 6, and 7), Burgener et al. (2022) did not observe an effect of ear punch location on seeding activity in white-tailed deer. Our finding of reduction in the AFR of samples collected from the ventral area of the elk ear is somewhat consistent with Ferreira et al. (2021), as our dorsal location is similar to location 6 in that publication. A statistically nonsignificant reduction in AFR was also observed in the central punch, which corresponds to position 1 or 7 in Ferreira et al. (2021). Collectively, these data have implications for elk tracking and herd management decisions. The opportunity cost of placing an ear tag where tissue is biopsied for CWD testing from the periphery of the elk ear may be reduced tracking efficacy, as tags may be more easily lost from the ear over the long term.

ACKNOWLEDGMENTS

The authors thank Tom Douville and Fred Schendel for assistance with all aspects of MNPROtein production. We thank Byron Buckley for critical review of the manuscript. ELISA tests were performed by staff at the South Dakota State University Animal Disease Research & Diagnostic Laboratory, Colorado State University Veterinary Diagnostic Laboratory, and Wyoming State Veterinary Laboratory. Funding was provided by the US Department of Agriculture (USDA) Animal and Plant Health Inspection Service (APHIS) Wild Cervid Chronic Wasting Disease (CWD) Management and Response Activities Program 2022 (#AP22WSNWRC00C056) and the Minnesota State Legislature through the Minnesota Legislative-Citizen Commission on Minnesota Resources (LCCMR). Conceptualization: S.S.L., A.S.N., Bryan J. Richards, S.L.G.; methodology, D.N.B., R.J.L.; data analysis: D.N.B., R.J.L., K.J.B., T.M.W., S.S.L.; writing, D.N.B., R.J.L., K.J.B., T.M.W., S.S.L.; editing: P.A.L., T.M.W., S.S.L.; funding: P.A.L., T.M.W., S.S.L.; D.N.B., A.S.N., A.J.L., S.L.G., K.J.B., T.M.W., S.S.L. declare no competing interests. P.A.L. is a cofounder and stock owner of Priogen Corp, a diagnostic company specializing in the ultrasensitive detection of pathogenic proteins associated with prion and protein-misfolding diseases. R.J.L. is an employee and stock owner of Priogen Corp. The University of Minnesota has licensed patent applications to Priogen Corp. Any use of trade, firm, or product names is for descriptive purposes only and does not imply endorsement by the US government.

SUPPLEMENTARY MATERIAL

Supplementary material for this article is online at http://dx.doi.org/10.7589/JWD-D-24-00071.

LITERATURE CITED

Budras KD, Habel RE. 2011. *Bovine anatomy*. Schlutersche, Hannover, Germany, 168 pp.

Burgener KR, Lichtenberg SS, Lomax A, Storm DJ, Walsh DP, Pedersen JA. 2022. Diagnostic testing of chronic wasting disease in white-tailed deer (*Odocoileus virginianus*) by RT-QuIC using multiple tissues. *PLoS One* 17:e0274531.

Carlson CM, Thomas S, Keating MW, Soto P, Gibbs NM, Chang H, Wiepz JK, Austin AG, Schneider JR, et al. 2023. Plants as vectors for environmental prion transmission. *iScience* 26:108428.

Carstensen B, Plummer M, Laara E, Hills M. 2023. Epi: Statistical analysis in epidemiology. https://cran.r-project.org/web/packages/Epi/index.html. Accessed March 2024.

Chiavacci SJ. 2022. The economic costs of chronic wasting disease in the United States. *PLoS One* 17:e0278366.

Denkers ND, Hoover CE, Davenport KA, Henderson DM, McNulty EE, Nalls AV, Mathiason CK, Hoover EA. 2020. Very low oral exposure to prions of brain or saliva origin can transmit chronic wasting disease. *PLoS One* 15:e0237410.

Dohoo I, Martin W, Stryhn H. 2009. *Veterinary epidemiologic research*. 2nd Ed. VER Incorporated, Charlottetown, PE, Canada, 890 pp.

Evans HE, de Lahunta A. 2012. *Miller's anatomy of the dog*. Elsevier, New York, New York, 1004 pp.

Ferreira NC, Charco JM, Plagenz J, Orru CD, Denkers ND, Metrick MA 2nd, Hughson AG, Griffin KA, Race B, et al. 2021. Detection of chronic wasting disease in mule and white-tailed deer by RT-QuIC analysis of outer ear. *Sci Rep* 11:7702.

Gilch S. 2022. Chronic wasting disease—A prion disease through a One Health lens. *Can Vet J Can Vet J* 63: 431–433.

Groveman BR, Williams K, Race B, Foliaki S, Thomas T, Hughson AG, Walters RO, Zou W, Haigh CL. 2024. Lack of transmission of chronic wasting disease to human cerebral organoids. *Emerg Infect Dis* 30:1193–1202.

Haley NJ, Siepker C, Hoon-Hanks LL, Mitchell G, Walter WD, Manca M, Monello RJ, Powers JG, Wild

MA, et al. 2016. Seeded amplification of chronic wasting disease prions in nasal brushings and rectoanal mucosa-associated lymphoid tissues from elk by real-time quaking-induced conversion. *J Clin Microbiol* 54:1117–1126.

Henderson DM, Denkers ND, Hoover CE, McNulty EE, Cooper SK, Bracchi LA, Mathiason CK, Hoover EA. 2020. Progression of chronic wasting disease in white-tailed deer analyzed by serial biopsy RT-QuIC and immunohistochemistry. *PLoS One* 15:e0228327.

Huang MHJ, Demarais S, Banda A, Strickland BK, Welch AG, Hearst S, Lichtenberg S, Houston A, Pepin KM, VerCauteren KC. 2024. Expanding CWD disease surveillance options using environmental contamination at deer signposts. *Ecol Solut Evid* 5:e12298.

Inzalaco HN, Bravo-Risi F, Morales R, Walsh DP, Storm DJ, Pedersen JA, Turner WC, Lichtenberg SS. 2023. Ticks harbor and excrete chronic wasting disease prions. *Sci Rep* 13:7838.

Johnson CJ, Pedersen JA, Chappell RJ, McKenzie D, Aiken JM. 2007. Oral transmissibility of prion disease is enhanced by binding to soil particles. *PLoS Pathog* 3:e93.

Johnson CJ, Phillips KE, Schramm PT, McKenzie D, Aiken JM, Pedersen JA. 2006. Prions adhere to soil minerals and remain infectious. *PLoS Pathog* 2:e32.

Keane D, Barr D, Osborn R, Langenberg J, O'Rourke K, Schneider D, Bochsler P. 2009. Validation of use of rectoanal mucosa-associated lymphoid tissue for immunohistochemical diagnosis of chronic wasting disease in white-tailed deer (*Odocoileus virginianus*). *J Clin Microbiol* 47:1412–1417.

Kim TY, Shon HJ, Joo YS, Mun UK, Kang KS, Lee YS. 2005. Additional cases of chronic wasting disease in imported deer in Korea. *J Vet Med Sci* 67:753–759.

Kuznetsova A, McKenzie D, Cullingham C, Aiken JM. 2020. Long-term incubation PrP^{CWD} with soils affects prion recovery but not infectivity. *Pathogens* 9:311.

Landis JR, Koch GG. 1977. The measurement of observer agreement for categorical data. *Biometrics* 33:159–174.

Lee YH, Sohn HJ, Kim MJ, Kim HJ, Lee WY, Yun EI, Tark DS, Cho IS, Balachandran A. 2013. Strain characterization of the Korean CWD cases in 2001 and 2004. *J Vet Med Sci* 75:95–98.

McNulty E, Nalls AV, Mellentine S, Hughes E, Pulscher L, Hoover EA, Mathiason CK. 2019. Comparison of conventional, amplification and bio-assay detection methods for a chronic wasting disease inoculum pool. *PLoS One* 14:e0216621.

Monaghan TF, Rahman SN, Agudelo CW, Wein AJ, Lazar JM, Everaert K, Dmochowski RR. 2021. Foundational statistical principles in medical research: Sensitivity, specificity, positive predictive value, and negative predictive value. *Medicina (Kaunas)* 57:503.

Opsahl RW. 2003. Chronic wasting disease of deer and elk: A call for national management. *Environ Law* 33:1059–1092.

Pepe MS. 2000. An interpretation for the ROC curve and inference using GLM procedures. *Biometrics* 56:352–359.

Pirisinu L, Tran L, Chiappini B, Vanni I, Di Bari MA, Vaccari G, Vikøren T, Madslien KI, Våge J, et al. 2018. Novel type of chronic wasting disease detected in moose (*Alces alces*), Norway. *Emerg Infect Dis* 24:2210–2218.

Pritzkow S, Morales R, Moda F, Khan U, Telling GC, Hoover E, Soto C. 2015. Grass plants bind, retain, uptake, and transport infectious prions. *Cell Rep* 11:1168–1175.

Prusiner SB. 1982. Novel proteinaceous infectious particles cause scrapie. *Science* 216:136–144.

R Core Team. 2024. *R: A language and environment for statistical computing*. R Foundation for Statistical Computing, Vienna, Austria. https://www.R-project.org/. Accessed March 2024.

Race BL, Meade-White KD, Ward A, Jewell J, Miller MW, Williams ES, Chesebro B, Race RE. 2007. Levels of abnormal prion protein in deer and elk with chronic wasting disease. *Emerg Infect Dis* 13:824–830.

Rashid Z, Davies AS, Steffert IJ. 1987. The anatomy of the auricular conchae of cattle, sheep and deer. *N Z Vet J* 35:144–149.

Robin X, Turck N, Hainard A, Tiberti N, Lisacek F, Sanchez JC, Müller M. 2011. pROC: an open-source package for R and S+ to analyze and compare ROC curves. *BMC Bioinform* 12:77.

Rowden GR, Picasso-Risso C, Li M, Schwabenlander MD, Wolf TM, Larsen PA. 2023. Standardization of data analysis for RT-QuIC-based detection of chronic wasting disease. *Pathogens* 12:309.

Schwabenlander MD, Rowden GR, Li M, LaSharr K, Hildebrand EC, Stone S, Seelig DM, Jennelle CS, Cornicelli L, et al. 2022. Comparison of chronic wasting disease detection methods and procedures: implications for free-ranging white-tailed deer (*Odocoileus virginianus*) surveillance and management. *J Wildl Dis* 58:50–62.

Seelig DM, Mason GL, Telling GC, Hoover EA. 2011. Chronic wasting disease prion trafficking via the autonomic nervous system. *Am J Pathol* 179:1319–1328.

Sim J, Wright CC. 2005. The kappa statistic in reliability studies: Use, interpretation, and sample size requirements. *Phys Ther* 85:257–268.

Soto P, Bravo-Risi F, Kramm C, Gamez N, Benavente R, Bonilla DL, Reed JH, Lockwood M, Spraker TR, et al. 2024. Nasal bots carry relevant titers of CWD prions in naturally infected white-tailed deer. *EMBO Rep* 25:334–350.

Spraker TR, Balachandran A, Zhuang D, O'Rourke KI. 2004. Variable patterns of distribution of PrP^{CWD} in the obex and cranial lymphoid tissues of Rocky Mountain elk (*Cervus elaphus nelson*) with subclinical chronic wasting disease. *Vet Rec* 155:295–302.

Spraker TR, VerCauteren KC, Gidlewski T, Schneider DA, Munger R, Balachandran A, O'Rourke KI. 2009. Antemortem detection of PrPCWD in preclinical, ranch-raised Rocky Mountain elk (*Cervus elaphus nelsoni*) by biopsy of the rectal mucosa. *J Vet Diagn Investig* 21:15–24.

Stsiapura VI, Maskevich AA, Kuzmitsky VA, Uversky VA, Kuznetsova IM, Turoverov KK. 2008. Thioflavin T as a molecular rotor: Fluorescent properties of thioflavin T in solvents with different viscosity. *J Phys Chem B* 112:15893–15902.

Sun JL, Kim S, Crowell J, Webster BK, Raisley EK, Lowe DC, Bian J, Korpenfelt SL, Benestad SL, Telling GC. 2023. Novel prion strain as cause of chronic wasting

disease in a moose, Finland. *Emerg Infect Dis* 29:323–332.

SVA (Swedish Veterinary Association). 2024. *CWD Surveillance Map*. Swedish Veterinary Association. https://www.sva.se/en/what-we-do/contagion-status/surveillance-of-chronic-wasting-disease-cwd/map-of-chronic-wasting-disease-cwd/. Accessed November 2024.

Tranulis MA, Tryland M. 2023. The zoonotic potential of chronic wasting disease—a review. *Foods* 12:824.

USDA (US Department of Agriculture), Animal and Plant Health Inspection Service. 2024. *NVAP reference guide: Chronic wasting disease (control and eradication)*. https://www.aphis.usda.gov/nvap/reference-guide/control-eradication/cwd. Accessed January 2024.

USGS (US Geological Survey). 2024. *Expanding distribution of chronic wasting diseases*. https://www.usgs.gov/centers/nwhc/science/expanding-distribution-chronic-wasting-disease?qt-science_center_objects=0#qt-science_center_objects. Accessed September 2024.

Wild MA, Spraker TR, Sigurdson CJ, O'Rourke KI, Miller MW. 2002. Preclinical diagnosis of chronic wasting disease in captive mule deer (*Odocoileus hemionus*) and white-tailed deer (*Odocoileus virginianus*) using tonsillar biopsy. *J Gen Virol* 83:2629–2634.

Will RG, Ironside JW, Zeidler M, Cousens SN, Estibeiro K, Alperovitch A, Poser S, Pocchiari M, Hofman A, Smith PG. 1996. A new variant of Creutzfeldt-Jakob disease in the UK. *Lancet* 347:921–925.

Williams ES, Young S. 1980. Chronic wasting disease of captive mule deer: A spongiform encephalopathy. *J Wildl Dis* 16:89–98.

Submitted for publication 27 April 2024.
Accepted 10 October 2024.